

Use of Isotope-Edited FTIR to Derive a Backbone Structure of a Transmembrane Protein

Joshua Manor,[†] Eyal Arbely,^{†,||} Andrè Beerlink,^{‡,⊥} Mutaz Akkawi,[§] and Isaiah T. Arkin^{*,†}

[†]Department of Biological Chemistry, The Alexander Silberman Institute of Life Sciences, The Hebrew University of Jerusalem, Edmund J. Safra Campus, Jerusalem 91904, Israel

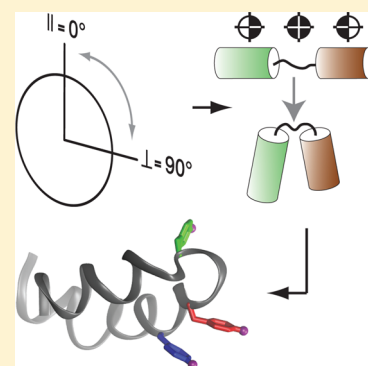
[‡]Institut für Röntgenphysik, Georg-August-Universität Göttingen, Friedrich-Hund-Platz 1, Göttingen 37077 Germany

[§]Faculty of Science and Technology, Al-Quds University, Abu Dis, Palestinian National Authority

Supporting Information

ABSTRACT: Solving structures of membrane proteins has always been a formidable challenge, yet even upon success, the results are normally obtained in a mimetic environment that can be substantially different from a biological membrane. Herein, we use noninvasive isotope-edited FTIR spectroscopy to derive a structural model for the SARS coronavirus E protein transmembrane domain in lipid bilayers. Molecular-dynamics-based structural refinement, incorporating the IR-derived orientational restraints points to the formation of a helical hairpin structure. Disulfide cross-linking and X-ray reflectivity depth profiling provide independent support of the results. The unusually short helical hairpin structure of the protein might explain its ability to deform bilayers and is reminiscent of other peptides with membrane disrupting functionalities. Taken together, we show that isotope-edited FTIR is a powerful tool to analyze small membrane proteins in their native environment, enabling us to relate the unusual structure of the SARS E protein to its function.

SECTION: Biophysical Chemistry and Biomolecules



The multiphasic environment in which membrane proteins reside provides a significant challenge to the structural biologist. X-ray crystallography is hindered by the difficulty in obtaining high-quality crystals. Solution-state NMR spectroscopy is hampered by the low tumbling rates of vesicles that are needed to solubilize the membrane protein. Hence both techniques that account for 98.9% of solved protein structures routinely require membrane mimetic agents, such as detergents to accomplish their task. Hence, it is of no surprise that membrane proteins comprise only 2.4% of the solved protein data bank, despite comprising 20–30% of known genomes.^{1,2}

In the current study, we attempt to use a new route to obtain structural models of membrane proteins using FTIR spectroscopy. As our target, we chose SARS coronavirus E-protein, given its importance and what seems to be its noncanonical features. An overview of SARS coronavirus and a comprehensive review of its E-protein are given in the Supporting Information.

Using linear dichroism isotope-edited FTIR spectroscopy, we determined the orientation of 19 carbonyl groups out of the 32 in the peptide. These restraints were subsequently used to obtain a structure for the protein by a molecular dynamics protocol employing experimental refinement.

It is worth pointing out that the use of isotope-edited FTIR to derive structural information on membrane proteins is similar in principle to solid-state NMR. Both methods can examine isotopically labeled peptides in lipid bilayers. However, the structural precision that is obtained by solid-state NMR in

comparison with the current study is significantly higher, yet the principal reasons that drove us to develop FTIR analysis as an alternative approach for structurally examining membrane peptides are the following: relatively low sample requirements (sub milligram), widespread instrumentation availability, short measurement time (few minutes), and ease of sample manipulation that enables multiple conditions to be tested (pH, ligand concentration, temperature, and lipid type, to name a few).

The result of our analysis is a unique helix–loop–helix motif that is consistent with the experimental data. Independent approaches were used to validate the structure, including disulfide cross-linking, X-ray reflectivity measurements, and H⁺/D⁺ exchange. It seems intriguing to assume that this uniquely short helix–loop–helix motif plays a major role in the peptide's capability to deform membranes and promote the budding process, reminiscent of other proteins that play a role in membrane destabilization.

The goal of our research plan was to obtain a reliable structural model of the SCoV-E protein transmembrane domain in lipid bilayers. The strategy was based on generating accurate experimental restraints that may be used in an objective model building process. Finally, additional exper-

Received: May 26, 2014

Accepted: July 15, 2014

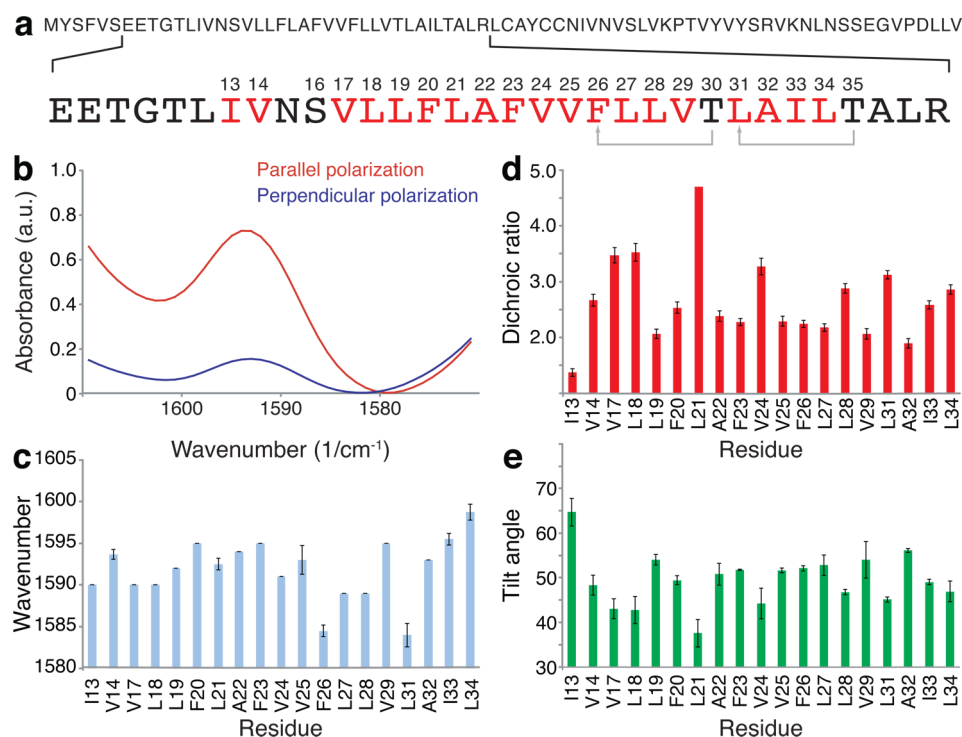


Figure 1. (a) Sequence of the SCov-E protein with the expanded region, E7-R38, indicating the transmembrane encompassing peptide used in all experiments. Red residues indicate positions of $^{13}\text{C}=\text{O}$ labeling. (b) Example FTIR spectra in the region of the isotope-edited amide I mode of a peptide labeled at L19. Spectra were obtained using parallel (red) or perpendicular (blue) polarized light. (c) Wavenumber of the isotope-edited $^{13}\text{C}=\text{O}$ amide I mode of the different residues. The positions are taken from the spectra shown in Supplementary Figure 1b in the Supporting Information. (d) Dichroic ratios of the amide I vibrational mode of the different $^{13}\text{C}=\text{O}$ labels in the SCov-E protein. (e) Tilt angles between the TDM of the amide I mode and the membrane normal derived from the respective dichroic ratios shown in panel d.

imental approaches were used to provide independent validation of the results.

As the subject for our investigation, we examined a peptide that encompasses the entire hydrophobic domain of SCov-E protein and corresponds to residues E7-R38 (Figure 1a). We have previously shown that this peptide exhibited properties that are indicative that a full structural investigation is warranted.³ In brief, the peptide was shown to be highly helical and fully embedded in the lipid bilayer. Moreover, the same peptide was shown to deform lipid vesicles, as expected from a protein that is involved in virus budding.⁴ Consequently, all of our studies were of the aforementioned transmembrane peptide of the SCov-E protein.

To derive accurate experimental restraints, we turned to isotope-edited FTIR spectroscopy. In brief, FTIR linear dichroism of $^{13}\text{C}=\text{O}$ labels provides an accurate measure of the tilt angle from the membrane normal of the transition dipole moment (TDM) of the respective amide I stretching mode.^{5–15} Because the geometry of the TDM of the amide I mode relative to the molecular frame is known,¹⁶ the measurements provide accurate orientational information on the labeled amide group. We note that severe sample mosaicity may interfere with the previous orientational analysis. However, when the Gaussian distribution of the mosaicity is below $\sigma = 5^\circ$, the effect of disorder is negligible.¹⁷ For this reason, FTIR analyses were accompanied by measurements of membrane mosaicity using X-ray reflectivity to ensure that sample disorder can be neglected.

Nineteen SCov-E transmembrane domain (TMD) peptides were synthesized, HPLC-purified, and reconstituted in lipid bilayers. Each peptide contained a single $^{13}\text{C}=\text{O}$ label

dispersed throughout the entire sequence of the peptide (Figure 1a). Virtually all spectra were comprised of α -helical amide I peaks and a negligible contribution from other conformations, namely, β -sheet, turns, and coils (data not shown), in agreement with previous work.³

The $^{13}\text{C}=\text{O}$ isotope-edited peak was found in all peptides (see example in Figure 1b) to be located between 1584 and 1601 cm^{-1} with an average peak center of $1592 \pm 4.6 \text{ cm}^{-1}$ (Figure 1c). In the majority of residues, the peak center was at 1590 cm^{-1} , as found in other helical peptides.^{6,9,10,13–15,18} However, two residues exhibited peaks that were shifted to significantly lower wavenumbers: F26 and L31 (peak center at $1584 \pm 0.3 \text{ cm}^{-1}$). This shift stems from the formation of a bifurcated H-bond geometry of the peptidic carbonyl and the hydroxyl group at residue at position $i + 4$.^{19,20} (See the gray connectors in Figure 1.)

Because this bifurcated H-bond pattern is indicative of an α -helical geometry, we can state that residues F26 to T35 are helical. This information provides further, site-specific secondary structure assignment to our previous study that showed that the SCov-E protein is on average predominantly helical.³ Finally, as detailed later, this information can be used to limit the position of any loop in the protein that resides between helical regions.

The first step to yield orientational restraints involved collection of linear dichroism spectra of the different peptides, a representative of which is shown in Figure 1b. All spectra are shown in Supplementary Figure 1 in the Supporting Information. Both parallel and perpendicular polarized spectra were obtained and fit as described in the Materials and

Methods section. The ratios between the two absorptions (a.k.a. dichroic ratios) are listed in Figure 1d.

It is possible to convert the dichroic ratios to angular information without consideration of sample disorder, as long as disorder is minimal.¹⁷ Therefore, the second step in our procedure was to use X-ray reflectivity rocking scans to measure the Gaussian distribution of each sample that was examined by FTIR spectroscopy. In all cases, the membrane mosaicity was below $\sigma = 5^\circ$, enabling us to neglect the effect of sample disorder when calculating the orientation of the amide I TDM orientation. An example of X-ray rocking a scan is shown in Supplementary Figure 2 in the Supporting Information.

After establishing that sample disorder is negligible, we could convert the measured dichroic ratios in Figure 1d to the tilt angles between the TDM of the amide I mode and the membrane normal, listed in Figure 1e. One can readily see that there is an inverse (albeit nonlinear) relationship between the dichroic ratio and the tilt angle: Larger dichroic ratios yield smaller tilt angles (e.g., L21), while smaller dichroic ratios yield more inclined tilt angles (e.g., I13). Finally, the experimentally derived tilt angles were used to derive an accurate model of the SCoV-E protein transmembrane domain using the molecular modeling approaches described later.

The first approach that we tried to employ was rigid body modeling, a procedure that may be used to model canonical transmembrane helices using orientational restraints.¹⁸ In brief, an ideal α -helix was constructed to match the sequence of the peptide used in this work. Initially the peptide was aligned with its director along the z axis. Following that, the peptide was tilted in 1° increments until it was completely inverted. At each tilt angle the peptide was rotated about its director by 1° increments until an entire revolution was obtained. All together, $64\,800 = 180 \times 360$ tilt and rotation combinations were created. Subsequently, at each tilt and rotation combination, the angles between the amide I TDMs of all 19 residues and the z axis of the resultant model were calculated. The measured angles were then compared with the experimentally derived values to see which spatial orientation of the peptide yields the best fit to the FTIR results.

As shown in Supplementary Figure 3 in the Supporting Information, the smallest difference between the TDM tilt angles of the experimental data and the results of the rigid body modeling is at tilt and rotation angles of 40 and 290° , respectively. However, the average difference of 14° per residue reflects a poor fit to the experimental data due to the fact that a rigid body fit to a set of random angles yields similar values (Supplementary Figure 3 in the Supporting Information). For comparison, the same procedure applied to a canonical helix, such as the M2 H⁺ channel from influenza A,¹⁸ yielded an average tilt angle difference of $<5^\circ$. Taken together, we conclude that the SCoV-E protein transmembrane domain does not adopt a canonical helix structure that is compatible with our experimental results.

Because our experimental results were inconsistent with a canonical helix structure, we set out to determine if a hairpin structure might exist. Toward this end, we tried to see if we can cross-link two distant parts of the protein that would only be close if the protein formed a hairpin structure. Two peptides were therefore synthesized, each with two cysteine residues. The first peptide contained the mutations S16C and T30C, while the second peptide contained the mutations S16C and T35C (Figure 2). All three residues (S16, T30, and T35) are found mutated in natural variants of the virus and are therefore

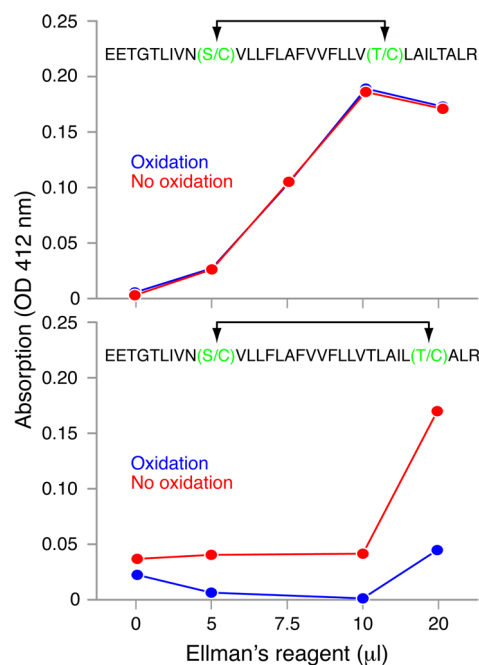


Figure 2. Results of the disulfide cross-linking experiments. Quantification of free thiols using Ellman's reagent (412 nm absorbance) as a function of reagent concentration. The blue line represents an oxidation experiment, while the red line depicts data without oxidation as control. Therefore, disulfide bond formation is observed when there is a difference between the two samples due to the fact the oxidation reduces the number of free thiols. The two panels present results for the two different peptides as indicated. The sequences of the peptides are shown on the top of every panel, indicating the cysteine mutations in green.

not expected to change the function nor the structure of the proteins.

To examine the proximity of the two mutated sites, we examined the ability of the two cysteine residues to form a disulfide bond. In brief, the peptides were reconstituted in lipid bilayers, followed by oxidation to promote disulfide bond formation. The reaction was then terminated, and the amount of free thiol groups was estimated. The results of the cross-linking experiments, shown in Figure 2, indicate a significant difference in the amount of free thiol between the two peptides. In particular, the peptide that contained the S16C and T35C mutations was capable of forming disulfide bonds, while the S16C and T30C containing peptide did not.

The results are incompatible with a parallel arrangement of an α -helical structure that places the two residues ~ 30 Å apart from one another. Rather, the results are supportive, albeit not conclusive of a hairpin model for SCoV-E protein in which residues S16 and T35 are in close proximity to one another. Therefore, to derive a reliable model for SCoV-E protein based on the FTIR data, we turned to MD-based refinement. Such an approach would allow conformational freedom to the resultant outcome while at the same time closer adherence to the experimental data.

A simulated annealing protocol was developed to incorporate the experimental restraints in an objective manner, alongside maintaining correct protein geometry.²¹ Two dummy atoms were placed in the peptide plane (Figure 3a), such that the bond between them coincided with the amide I TDM.¹⁶ Therefore, harmonically restraining the bond between these

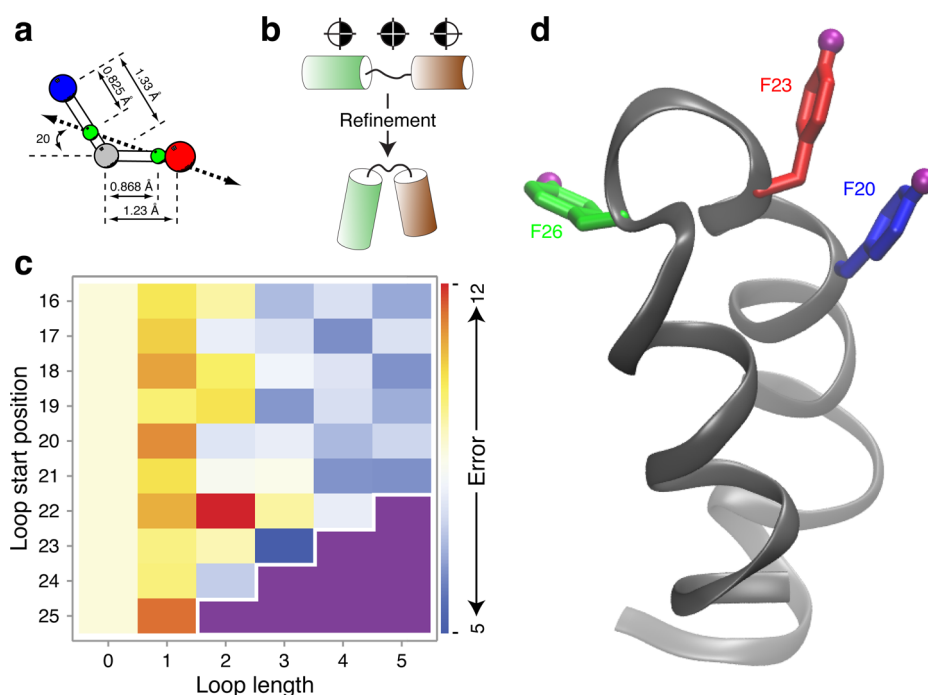


Figure 3. (a) Diagram of the orientation of the TDM of the amide I mode relative to the amide group's molecular geometry.¹⁶ The two dummy atoms that were used in the refinement process are shown in green. The dotted arrow represents the amide I TDM. (b) Schematic of the refinement process showing the quadrants of the angular restraints that were imposed during the simulation. In the first helix (green), the angles were restrained to $\pm\theta$, while in the second helix (brown) they were restrained to $\pi \pm\theta$. In the region between the two helices the angle were refined to any of the four possible quadrants. (c) Results of the refinement process: 40 different simulations were run, each differing in the loop size (1 to 5 residues) and position (starting from residue 16 to 25). A continuous helix is signified by a loop length of 0 (left column). The color scale represents the TDM tile angle difference per residue that the resulting structure has relative to the data derived from the FTIR study. The combinations shown in purple were not tested. (d) Structure of the SCov-E protein obtained from experimental refinement depicting the position of the three labeled phenylalanines, as indicated in Figure 4. The positions of the iodines are shown in purple.

two atoms to a particular angle relative to the z axis corresponded to refinement based on the experimental data.

One important consideration in the previously described refinement procedure relates to the fact that the measured absorption is proportional to the squared scalar product of the electric field vector and the TDM. Hence, there is an angular ambiguity between the four different quadrants regarding the position of the actual angle measured: The FTIR-based experiment cannot distinguish between θ , $-\theta$, $\pi + \theta$, or $\pi - \theta$ (quadrants I, IV, III, and II, respectively). Therefore, our energy function was designed such that it does not distinguish between the four angles as well.

Initial refinement trials have shown that movements between the four quadrants rarely occurred due to entrapment in local minima. As a result, a complete unbiased refinement based on the experimental restraints would not be feasible. However, because the protein was shown to be highly helical in our work and in previous studies,^{3,22,23} we could introduce the following simplifying assumption: All TDM tilt angles in a mildly inclined, continuous helix will either be in the right hemisphere ($\pm\theta$) or left hemisphere ($\pi \pm\theta$). The reason for this geometric fact is that in an α -helix the angle between the TDM and the helix axis is relatively small (ca. 35° ¹⁶). The reader is referred to previous studies^{5,17,24} for a comprehensive treatment describing the geometry of the TDM as a function of helix tilt and uniaxial rotation.

On the basis of the above, we proceeded to model the protein as predominantly helical with a stretch of nonhelical residues of varying length and position. Hence, the protein

contained three segments: two helical stretches interspersed by a nonhelical segment. The location of the nonhelical stretch was estimated to be anywhere between residues S16 and V25. The reason being is that the flanking stretches were shown to be helical based on the shift in the amide I frequency due to intrahelical H-bonding previously discussed. (See the gray arrows in Figure 1.)

Helical stretches were maintained using harmonic restraints between every carbonyl oxygen of residue i and the amide H⁺ at position of $i + 4$. The orientational refinement was imposed by allowing the TDM tilt angle to converge only to one hemisphere: $\pm\theta$ in the case of an upward pointing helix or $\pi \pm\theta$ in the case of a downward pointing helix. In the nonhelical segment, the angular restraints were allowed to converge to any of the four quadrants.

The disulfide cross-linking experiments as well as previous independent experiments³ have shown that the protein adopts a hairpin structure. Therefore, the orientational restraints in the two helical stretches were set to opposite hemispheres. (See the schematic in Figure 3b.) In the final step of the refinement process, after the orientational refinement took place, the results of the disulfide cross-linking experiments were imposed. The procedure involved a simple harmonic distance restraint between the C β atoms of S16 and T35.

The refinement program employed nonhelical segments ranging in lengths from one to five residues. In addition, the starting location of the nonhelical segment was shifted from residue 10 to 19. In total, 40 simulations were conducted of varying loop length and position. The success of each

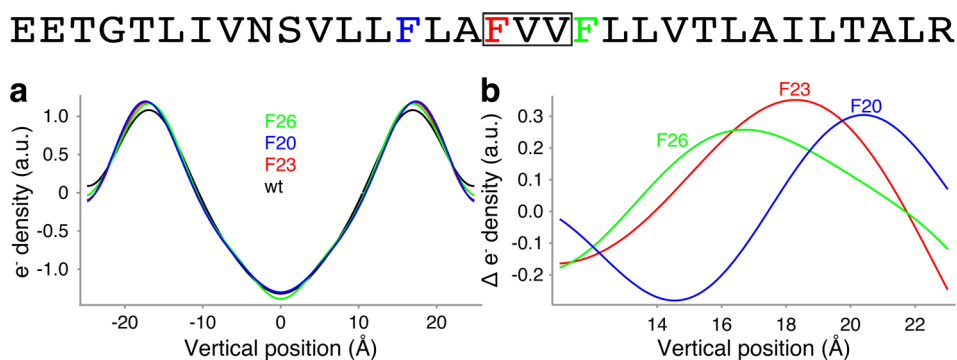


Figure 4. X-ray reflectivity depth profiling of the SCoV-E protein in lipid bilayers. The sequence of the peptide indicating the positions of the different *para*-iodo-phenylalanine in color is shown at the top. The boxed residues (F23–V25) are the location of the loop in the model that was obtained after orientational refinement. (a) Electron density profiles as a function of the bilayer vertical position resulting from the reflectivity curves shown in Supplementary Figure 4 in the Supporting Information. (b) Difference electron density profiles between the iodinated samples and the unlabeled protein.

refinement simulation was evaluated by comparing the TDM tilt angles of the resultant structures to the experimental data using quadrant-independent difference. Finally, for comparative purposes, a refinement simulation in which the entire segment was treated as helical was conducted.

As shown in Figure 3c, the lowest angular deviation from the experimental results occurred with a protein containing a loop of three amino acids starting at residue F23. The TDM tilt angle difference per residue of this structure relative to the tilt angles derived from the FTIR is 5.3° . In comparison, the angular difference between experiment and refinement when simulating the protein as one long helix was much larger, 8.7° (see loop length 0: Figure 3c, left column). This value is very similar to the average difference of 8.3° obtained in all simulations. Hence, the MD refinement procedure was able to yield a structure that is in close agreement with the orientational data and still abides by the cross-linking restraints. In addition, both refinement procedures, MD and rigid body modeling, were inconsistent with a uniform helical structure of the SCoV-E protein.

To validate the structural model of the SCoV-E protein transmembrane domain that was obtained based on the FTIR data, we turned to independent data: the vertical position of the three phenylalanine residues, as determined by electron density profiling using X-ray reflectivity. The electron density profile of two very similar samples is compared: wild-type SCoV-E protein in hydrated lipid bilayers and precisely the same system except for the fact that the protein contained a *para*-iodinated phenylalanine instead of the regular phenylalanine. Iodination did not perturb any of the properties of the protein that we could measure. Consequently, the difference between the electron density profile of the two samples points to the vertical location of the iodine relative to the bilayer center. In our previous study on SCoV-E protein, we used this approach to pinpoint the position of F23.³ In the current study, we extended the previously described approach to determine the vertical position of the two other phenylalanine residues, F20 and F26, alongside a repeat analysis of F23.

As shown in Figure 4a, all SCoV-E protein variants embedded in a hydrated lipid bilayer exhibited the following electron density profile: The center of the lipid bilayer displays the lowest electron density due to the lipid methyl groups. In contrast, located ca. 18 Å from the bilayer center, we find the regions with the highest electron density that correspond to the

lipid headgroup. Subtraction of the wild-type electron density profile from that obtained from the three labeled samples reveals the location of the iodine relative to bilayer center: 20.5, 18.5, and 16.9 Å for F20, F23, and F26, respectively (Figure 4b).

In the hairpin model that we have derived based on the FTIR orientational restraints, there is loop starting from residue F23 to V25. (See the boxed residues in Figure 4.) These locations are entirely consistent with a transmembrane helical hairpin model in that all three residues are either in the loop or very close to it (Figure 3d). Hence, their position close to the lipid headgroup region is predicted by the model and confirmed by the X-ray reflective electron density profiling.

Traditionally, FTIR dichroism was used to infer the geometrical positioning of a known rigid structure, that is, the tilt and rotation angles of an α helix.^{5–15} This procedure involves spatial rotation and tilt of the helices until the back-calculated orientational restraints match best those that were obtained experimentally. Even though FTIR-derived tilt angles represent the average tilt and rotation angles of individual peptides, a successful construction of an α -helix using rigid body refinement is a strong indicator of a canonical form for a helical peptide. In influenza's M2 H⁺ channel, this rapid procedure had shown a great degree of accuracy, relying on FTIR angles alone.¹⁸

In the current study, we use site-directed dichroism on the SCoV-E protein. However, when we employed the same procedures used in the past, we were not successful. In particular, modeling the protein as a continuous helix yielded a structure that did not conform to the experimental restraints. While the role of rigid body refinement is quite limited, failing to reconstruct a continuous helix with a better agreement to the experimental results than to a set of random angles greatly reduces the possibility for such a conformation. Hence, a different approach to structural refinement was needed, akin to the way data are used in distance geometry in solution NMR spectroscopy.

Toward this end, we developed an MD-based protocol that employed the orientational data as a refinement criteria. However, because the number of structural degrees of freedom far outnumbers the orientational data points, additional structural information was required. Here we could make use of the secondary structure information that is available from FTIR, which allowed us to constrain certain parts of the protein

as helical. In search of an intrahelical motif, middle residues in the peptide were allowed to move more freely, including the local unwinding of the helix. Significant wavenumber shifts in site-specific peaks were used to define the helical constraints and narrow down the intrahelical motif search. It is not clear whether a smaller degree of wavenumber shifts should account for residues lining the motif. Together, the approach yielded a helical hairpin structure that corresponded well to the experimental data. Finally, to the best of our knowledge, this is the first time a molecular dynamics protocol is combined with FTIR linear dichroism studies to suggest a secondary structure of a peptide, which seems far from a canonical helix.

The hairpin structure model is supported independently by several lines of evidence, some provided in the current study and others in previous work. In the current study, we show using electron density depth profiling that the three middle phenylalanines are located near the headgroup region of the lipid bilayer. These residues, F20, F23, and F26, are placed right around the loop in our hairpin structure, which is between amino acids 23 to 25. (See Figure 1a.) This is entirely consistent with their close vertical location, which is $<4 \text{ \AA}$ apart. In contrast, if the protein was a continuous helix, the vertical distance between the three residues was 9 \AA . Tilting of the helix would reduce the vertical distance between the residues, but to reach a value of 4 \AA would necessitate a tilt of 64° . Such a tilt is not supported by the linear dichroism data.^{3,22,23} In addition, the depth profiling maintains that the three phenylalanines, which are in the middle of the hydrophobic stretch of the protein, are located near the lipid headgroup region. Hence, if the protein was a continuous helix, it would mean that half of the protein residues are outside of the bilayer. This is inconsistent with amide H^+/D^+ results that show that the majority of the protein is embedded in the lipid bilayer.³ We do recognize that rotamer flexibility might impact the vertical position of the residues because the label is located on the side chain. However, the extent of uncertainty in the vertical position of the iodinated side-chains is at most a few angstroms. Therefore, it is not sufficient to counter the central geometric argument that places three phenylalanines close to the lipid headgroup region and not in the middle of the lipid bilayer.

Another line of evidence to support the hairpin structure in the current study is disulfide cross-linking. Our results point to close proximity between residues S16 and T39, entirely incompatible with a continuous helix where they would be located $\sim 34 \text{ \AA}$ apart. Finally, using topology analyses, other laboratories have shown that the termini of coronavirus E proteins to be either on the same side of the membrane²⁵ or on opposite sides. In SCoV-E protein, the majority of the protein exhibited a topology in which both termini residues were on the same side of the membrane,²⁶ which is consistent with a hairpin structure.

While it is difficult to conclusively point to the mechanism of viral budding from the structural model that we obtained, one interesting finding arises: The helical hairpin structure of SCoV-E protein is similar to that of the influenza haemagglutinin fusion domain.^{27,28} The fusion domain contains two short helices of ten and eight residues connected by a very short loop. If one considers that the hydrophobic thickness of a lipid bilayer is $\sim 30 \text{ \AA}$, it is obvious that the influenza haemagglutinin fusion domain cannot traverse the entire length of the bilayer. Therefore, one may speculate that its insertion into the bilayer causes destabilization with the eventual fusion between the endocytic and viral membrane. Similarly, in the

model that we obtained for SCoV-E protein there are also two short helices, 16 and 12 residues in length. This is remarkable because like the influenza haemagglutinin, SCoV-E protein may partake in lipid destabilization during the viral budding process.

MATERIAL AND METHODS

The detailed procedures employed in the study are given in the Supporting Information. In brief, the experimental procedures used to synthesize the SCoV-E protein peptide and to collect the FTIR data are described in ref 3. Peak fitting and integration are described in ref 29. The procedures used in the X-ray reflectivity depth profiling are undertaken as described in refs 3, 17, 30, and 31. Molecular modeling using rigid body analysis was as described in ref 18, while MD-based refinements are described in detail in ref 21. Disulfide cross-linking has not been previously described by us and is therefore fully detailed in the Supporting Information. In brief, two peptides were synthesized, each with a pair of cysteine mutations: S16C+T35C or S16C+T30C. Both peptides were reconstituted in lipid bilayers and exposed to an oxidation catalyst. Experiments with an inactivated catalyst served as control. Finally, the level of disulfide bond formation was examined by comparing remaining free thiols in the control and experiment using Ellman's reagent.

ASSOCIATED CONTENT

Supporting Information

Background on the SARS coronavirus. Background on the functional and structural studies of the coronavirus E protein. Figure showing the FTIR spectra in the region of the isotope-edited amide I mode of the different labeled peptides in hydrated lipid bilayers. Figure showing the membrane mosaicity measurement using X-ray reflectivity. Figure showing the results of the rigid body modeling of the SCoV-E protein transmembrane domain. Detailed description of the material and methods used. This material is available free of charge via the Internet at <http://pubs.acs.org>.

AUTHOR INFORMATION

Corresponding Author

*E-mail: arkin@huji.ac.il

Present Addresses

^{||}E.A.: Department of Chemistry, Ben-Gurion University of the Negev, Beer-Sheva, 84105, Israel.

¹A.B.: Incoatec GmbH, Max-Planck-Strasse 2 Geesthacht, 21502, Germany.

Notes

The authors declare no competing financial interest.

ACKNOWLEDGMENTS

This work was partially supported by grants from the Binational Science Foundation (2008035), the Israeli science foundation (1581/08 and 175/13), the Deutsche Forschungsgemeinschaft, and by a grant from Niedersachsen. We thank Prof. Dr. Tim Salditt from Georg-August-Universität for helpful discussions. I.T.A. is the Arthur Lejwa Professor of Structural Biochemistry at the Hebrew University of Jerusalem.

REFERENCES

- (1) Stevens, T. J.; Arkin, I. T. Do More Complex Organisms Have a Greater Proportion of Membrane Proteins in Their Genomes? *Proteins: Struct., Funct., Genet.* **2000**, *39*, 417–420.

- (2) Krogh, A.; Larsson, B.; von Heijne, G.; Sonnhammer, E. L. Predicting Transmembrane Protein Topology with a Hidden Markov Model: Application to Complete Genomes. *J. Mol. Biol.* **2001**, *305*, 567–580.
- (3) Arbely, E.; Khattari, Z.; Brotons, G.; Akkawi, M.; Salditt, T.; Arkin, I. T. A Highly Unusual Palindromic Transmembrane Helical Hairpin Formed by SARS Coronavirus E Protein. *J. Mol. Biol.* **2004**, *341*, 769–779.
- (4) Siu, Y. L.; Teoh, K. T.; Lo, J.; Chan, C. M.; Kien, F.; Escriou, N.; Tsao, S. W.; Nicholls, J. M.; Altmeyer, R.; Peiris, J. S. M.; et al. The M, E, and N Structural Proteins of the Severe Acute Respiratory Syndrome Coronavirus Are Required for Efficient Assembly, Trafficking, and Release of Virus-Like Particles. *J. Virol.* **2008**, *82*, 11318–11330.
- (5) Arkin, I.; MacKenzie, K.; Brunger, A. Site-Directed Dichroism as a Method For Obtaining Rotational and Orientational Constraints for Oriented Polymers. *J. Am. Chem. Soc.* **1997**, *119*, 8973–8980.
- (6) Arkin, I. T. Isotope-edited IR spectroscopy for the study of membrane proteins. *Curr. Opin. Chem. Biol.* **2006**, *10*, 394–401.
- (7) Kukol, A.; Arkin, I. T. Structure of the Influenza C Virus CM2 Protein Transmembrane Domain Obtained by Site-Specific Infrared Dichroism and Global Molecular Dynamics Searching. *J. Biol. Chem.* **2000**, *275*, 4225–4229.
- (8) Kukol, A.; Arkin, I. T. *vpu* Transmembrane Peptide Structure Obtained by Site-Specific Fourier Transform Infrared Dichroism and Global Molecular Dynamics Searching. *Biophys. J.* **1999**, *77*, 1594–1601.
- (9) Kukol, A.; Torres, J.; Arkin, I. T. A Structure for the Trimeric MHC Class II-Associated Invariant Chain Transmembrane Domain. *J. Mol. Biol.* **2002**, *320*, 1109–1117.
- (10) Torres, J.; Kukol, A.; Goodman, J. M.; Arkin, I. T. Site-Specific Examination of Secondary Structure and Orientation Determination in Membrane Proteins: The Peptidic (13)C=(18)O Group As a Novel Infrared Probe. *Biopolymers* **2001**, *59*, 396–401.
- (11) Torres, J.; Kukol, A.; Arkin, I. T. Use of a Single Glycine Residue to Determine the Tilt and Orientation of a Transmembrane Helix. A New Structural Label for Infrared Spectroscopy. *Biophys. J.* **2000**, *79*, 3139–3143.
- (12) Torres, J.; Adams, P. D.; Arkin, I. T. Use of a New Label, (13)C=(18)O, in the Determination of a Structural Model of Phospholamban in a Lipid Bilayer. Spatial Restraints Resolve the Ambiguity Arising from Interpretations of Mutagenesis Data. *J. Mol. Biol.* **2000**, *300*, 677–685.
- (13) Torres, J.; Briggs, J. A. G.; Arkin, I. T. Convergence of Experimental, Computational and Evolutionary Approaches Predicts the Presence of a Tetrameric Form for CD3-Zeta. *J. Mol. Biol.* **2002**, *316*, 375–384.
- (14) Torres, J.; Briggs, J. A. G.; Arkin, I. T. Multiple Site-Specific Infrared Dichroism of CD3-Zeta, A Transmembrane Helix Bundle. *J. Mol. Biol.* **2002**, *316*, 365–374.
- (15) Torres, J.; Arkin, I. T. C-Deuterated Alanine: A New Label to Study Membrane Protein Structure Using Site-Specific Infrared Dichroism. *Biophys. J.* **2002**, *82*, 1068–1075.
- (16) Torii, H.; Tasumi, M. Model-Calculations on the Amide-I Infrared Bands of Globular-Proteins. *J. Chem. Phys.* **1992**, *96*, 3379–3387.
- (17) Manor, J.; Khattari, Z.; Salditt, T.; Arkin, I. T. Disorder Influence on Linear Dichroism Analyses of Smectic Phases. *Biophys. J.* **2005**, *89*, 563–571.
- (18) Manor, J.; Mukherjee, P.; Lin, Y.-S.; Leonov, H.; Skinner, J. L.; Zanni, M. T.; Arkin, I. T. Gating Mechanism of the Influenza A M2 Channel Revealed by 1D and 2D IR Spectroscopies. *Structure* **2009**, *17*, 247–254.
- (19) Gray, T. M.; Matthews, B. W. Intrahelical Hydrogen Bonding of Serine, Threonine and Cysteine Residues within Alpha-Helices and Its Relevance to Membrane-Bound Proteins. *J. Mol. Biol.* **1984**, *175*, 75–81.
- (20) Feldblum, E. S.; Arkin, I. T. Experimental Measurement of the Strength of a Bifurcated H-Bond. *Proc. Natl. Acad. Sci. U.S.A.* **2014**, *111*, 4085–4090.
- (21) Manor, J.; Arkin, I. T. Gaining Insight into Membrane Protein Structure Using Isotope-Edited FTIR. *Biochim. Biophys. Acta* **2012**, *1828*, 2256–2264.
- (22) Shen, X.; Xue, J.-H.; Yu, C.-Y.; Luo, H.-B.; Qin, L.; Yu, X.-J.; Chen, J.; Chen, L.-L.; Xiong, B.; Yue, L.-D.; et al. Small Envelope Protein E of SARS: Cloning, Expression, Purification, CD Determination, and Bioinformatics Analysis. *Acta Pharmacol. Sin.* **2003**, *24*, 505–511.
- (23) Parthasarathy, K.; Ng, L.; Lin, X.; Liu, D. X.; Pervushin, K.; Gong, X.; Torres, J. Structural Flexibility of the Pentameric SARS Coronavirus Envelope Protein Ion Channel. *Biophys. J.* **2008**, *95*, L39–L41.
- (24) Kass, I.; Arbely, E.; Arkin, I. T. Modeling Sample Disorder in Site-Specific Dichroism Studies of Uniaxial Systems. *Biophys. J.* **2004**, *86*, 2502–2507.
- (25) Maeda, J.; Repass, J. F.; Maeda, A.; Makino, S. Membrane Topology of Coronavirus E Protein. *Virology* **2001**, *281*, 163–169.
- (26) Yuan, Q.; Liao, Y.; Torres, J.; Tam, J. P.; Liu, D. X. Biochemical Evidence for the Presence of Mixed Membrane Topologies of the Severe Acute Respiratory Syndrome Coronavirus Envelope Protein Expressed in Mammalian Cells. *FEBS. Lett.* **2006**, *580*, 3192–3200.
- (27) Lorieau, J. L.; Louis, J. M.; Schwieters, C. D.; Bax, A. pH-Triggered, Activated-State Conformations of the Influenza Hemagglutinin Fusion Peptide Revealed by NMR. *Proc. Natl. Acad. Sci. U.S.A.* **2012**, *109*, 19994–19999.
- (28) Lorieau, J. L.; Louis, J. M.; Bax, A. The Complete Influenza Hemagglutinin Fusion Domain Adopts a Tight Helical Hairpin Arrangement at the Lipid:Water Interface. *Proc. Natl. Acad. Sci. U.S.A.* **2010**, *107*, 11341–11346.
- (29) Manor, J.; Feldblum, E. S.; Zanni, M. T.; Arkin, I. T. Environment Polarity in Proteins Mapped Noninvasively by FTIR Spectroscopy. *J. Phys. Chem. Lett.* **2012**, *3*, 939–944.
- (30) Khattari, Z.; Arbely, E.; Arkin, I. T.; Salditt, T. Viral Ion Channel Proteins in Model Membranes: A Comparative Study by X-ray Reflectivity. *Eur. Biophys. J.* **2006**, *36*, 45–55.
- (31) Khattari, Z.; Brotons, G.; Akkawi, M.; Arbely, E.; Arkin, I. T.; Salditt, T. SARS Coronavirus E Protein in Phospholipid Bilayers: An X-ray Study. *Biophys. J.* **2006**, *90*, 2038–2050.